

# Supplementary Material for "Fabrication and Characterization of Aluminum Airbridges for Superconducting Microwave Circuits"

Zijun Chen,<sup>1</sup> A. Megrant,<sup>1,2</sup> J. Kelly,<sup>1</sup> R. Barends,<sup>1</sup> J. Bochmann,<sup>1</sup> Yu Chen,<sup>1</sup> B. Chiaro,<sup>1</sup> A. Dunsworth,<sup>1</sup> E. Jeffery,<sup>1</sup> J.Y. Mutus,<sup>1</sup> P.J.J. O'Malley,<sup>1</sup> C. Neill,<sup>1</sup> P. Roushan,<sup>1</sup> D. Sank,<sup>1</sup> A. Vainsencher,<sup>1</sup> J. Wenner,<sup>1</sup> T.C. White,<sup>1</sup> A.N. Cleland,<sup>1,3</sup> and John M. Martinis<sup>1,3, a)</sup>

<sup>1)</sup> *Department of Physics, University of California, Santa Barbara, California 93106-9530, USA*

<sup>2)</sup> *Department of Materials, University of California, Santa Barbara, California 93106, USA*

<sup>3)</sup> *California NanoSystems Institute, University of California, Santa Barbara, CA 93106-9530, USA*

(Dated: January 16, 2014)

We provide supplementary data and calculations, primarily for practical design considerations when building superconducting circuits using airbridges. We also show a sample calculation of the contribution of an airbridge to microwave loss.

## I. IMPROVEMENT OF QUBIT COHERENCE USING CROSSOVERS

As described in Ref 1, we have previously measured energy relaxation times  $T_1$  (related to the resonator quality factor by  $T_1 = Q/\omega$ ) as a function of frequency for tunable superconducting Josephson qubits built in an architecture similar to the CPW resonators described in the main paper. The qubits we measured had a range of center trace widths  $S$  and gap widths  $W$ , from  $S = 8 \mu\text{m}$  and  $G = 8 \mu\text{m}$  up to  $S = 24 \mu\text{m}$  and  $G = 24 \mu\text{m}$ . As expected from considerations of surface loss due to two-level system defects, qubits with larger gap widths generally had increased energy relaxation times. However, the larger qubits also tended to have large frequency ranges where the  $T_1$  was suppressed, compared to smaller qubits where regions of suppressed  $T_1$  were limited to sharp peaks.

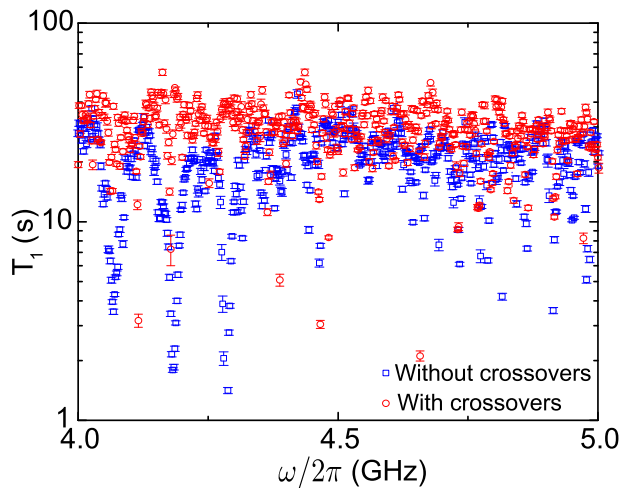


Figure 1. (Color online):  $T_1$  versus frequency for a tunable Josephson qubit, with center trace width and gap width both  $24 \mu\text{m}$ , (a) with dielectric crossovers and (b) without crossovers. Details of the measurement can be found in Ref 1.

The  $T_1$  versus frequency data for the largest of these qubits from Ref. 1 is shown in blue squares in Fig. 1. We hypothesize that these large regions of suppressed  $T_1$  were caused by radiation to slotline modes present in the control lines and readout resonators. Larger qubits are more susceptible to these modes because these modes can be capacitively coupled to the qubit, and the only effort made to suppress these modes on this chip was to wirebond discontinuous ground planes. To more effectively address this problem, we fabricated qubits nominally identical to the largest qubit measured in Ref 1 ( $S, W = 24 \mu\text{m}$ ), but with the addition of aluminum crossovers supported by 200 nm of  $\text{SiO}_2$ .<sup>2</sup> The insulator support structure of these crossovers would dominate the losses of resonators and qubits, but have minimal effect when placed on control lines. The resulting data is shown in red circles in Fig. 1, which compared to the data from Ref. 1, shows none of the large regions of  $T_1$  suppression.

## II. ESTIMATION OF AIRBRIDGE CRITICAL CURRENT

As detailed in the main paper, we fabricated 10 airbridges in series and measured them in a four terminal configuration. Each airbridge had a width of  $8 \mu\text{m}$ , a length of  $28 \mu\text{m}$ , and a thickness of 300 nm. At room temperature, we measured a resistance of  $6 \Omega$ . For a standard aluminum resistivity of  $2.7 \times 10^{-6} \Omega\text{-cm}$ , the expected resistance at room temperature is  $3.15 \Omega$ , which does not take into account the curvature of the bridges and the distance between the pads of the bridges, which was 6 microns. At 100 mK, we were limited to 10 mA of drive current, which was not enough to drive the airbridges normal. Instead, we slowly cooled the sample through the critical temperature  $T_c$  and measured the critical current  $I_c$  of the airbridges as a function of temperature just below  $T_c$ , with the results shown in Fig. 2. The critical temperatures for both the base wiring and the airbridge layer were within 50 mK of each other, and were around 1.2 K. The critical current data matches the

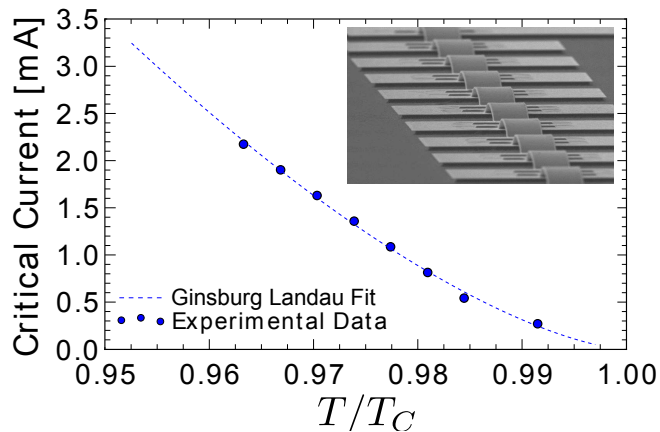


Figure 2. (Color online): Inset: Ten airbridges fabricated in series for a four terminal measurement of the resistance. Main panel: Critical current as a function of reduced temperature  $T/T_c$ . The fit is to Eqn. 1, with  $I_0 = 462$  mA

expected Ginsburg-Landau behavior, which predicts the following relation for the critical current of a thin superconducting wire<sup>3</sup>

$$I_c = I_0 (1 - T/T_c)^{2/3} \quad (1)$$

where  $I_0$  is the critical current at temperature well below  $T_c$ . By fitting to this equation, we extracted a low temperature critical current of 462 mA. However, this result does not take into account the width of our airbridges. From previous works, we estimate that there is a decrease in  $I_0$  by a factor of order 3 or 4 for an  $8 \mu\text{m}$  wire,<sup>4,5</sup> giving a critical current of around 100 mA.

### III. SHIFTS IN RESONANT FREQUENCY DUE TO AIRBRIDGES

Compared to more conventional crossovers which are supported by dielectrics, airbridges have a much smaller impact on the capacitance of a CPW line. However, this additional capacitance due to an airbridge is not negligible and should be accounted for. For example, in our experiment to test the microwave loss of airbridges using ten different resonators, we designed the resonators such that the density of airbridges increased with decreasing frequency, as shown in Fig. 3(a). A higher density of airbridges increases the capacitance of the resonator and decreases the resonant frequency. Thus, in our experiment, the resonant frequencies shifted further apart rather than closer together, avoiding any frequency collisions. We note here that from our control data, we found no significant correlation of the high or low power quality factor with the frequency of the resonator over the range we considered, which validated this particular design choice.

If we assume the airbridge acts like a parallel plate capacitor between the center trace and ground, we can es-

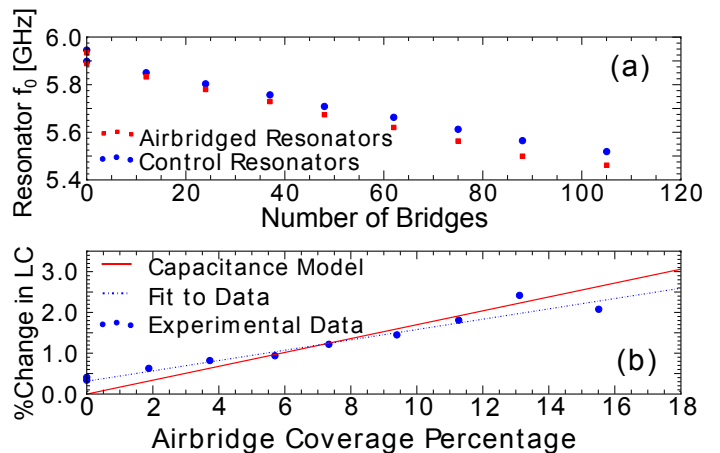


Figure 3. (Color online): (a) Resonant frequencies for resonators with variable numbers of airbridges in red squares, compared with the frequencies of their corresponding controls which are designed to have the same length. As the number of bridges increases, the resonators shift lower in frequency compared to their controls. (b) Percent change in  $LC$ , the product of the inductance per length and capacitance per length, as a function of the percentage of the resonator covered by airbridges. The dashed blue line is a linear fit to the data, with slope 12.7% and intercept 0.35%. The offset from the origin is within normal chip to chip variations in our measured resonators. The red line is a prediction based on the additional capacitance of the airbridge. The slopes differ due to the decrease in inductance from the airbridge.

timate the additional capacitance per unit length due to the airbridge as  $C = \epsilon_0 w/d$ , where  $w$  is the width of the center trace and  $d$  is the height of the airbridge. For the geometry in our experiment,  $w = 10 \mu\text{m}$  and  $d = 3 \mu\text{m}$ , giving  $C = 29.5$  pF/m. We can also numerically calculate the additional capacitance due to the airbridge using COMSOL. We simulated the cross-section of a CPW line with a  $10 \mu\text{m}$  center trace and  $5 \mu\text{m}$  gap with a substrate dielectric constant of 11.6, and found the capacitance per length to be 175.25 pF/m. After adding an airbridge, the capacitance increased to 204.03 pF/m giving an increase of 28.78 pF/m due to the airbridge, showing remarkable agreement with the parallel plate estimate. From these values, we predict that the capacitance of a resonator covered completely by airbridges should increase by 17%.

From the frequency data shown in Fig. 3(a), we can determine the actual effect of placing an airbridge over a CPW line. As the number of airbridges increased, the frequency of the resonator shifted further below the frequency of its corresponding control. Since each resonator and its control are designed to have the same wavelength, we can interpret the change in frequency as a change in the phase velocity of light  $v_p = 1/\sqrt{LC}$ , where  $L$  and  $C$  are the inductance and capacitance per unit length. Given the total length of the resonator and the number of airbridges, we can also determine the percentage of the line covered by airbridges. The percent coverage should be linearly related to the change in the product of the

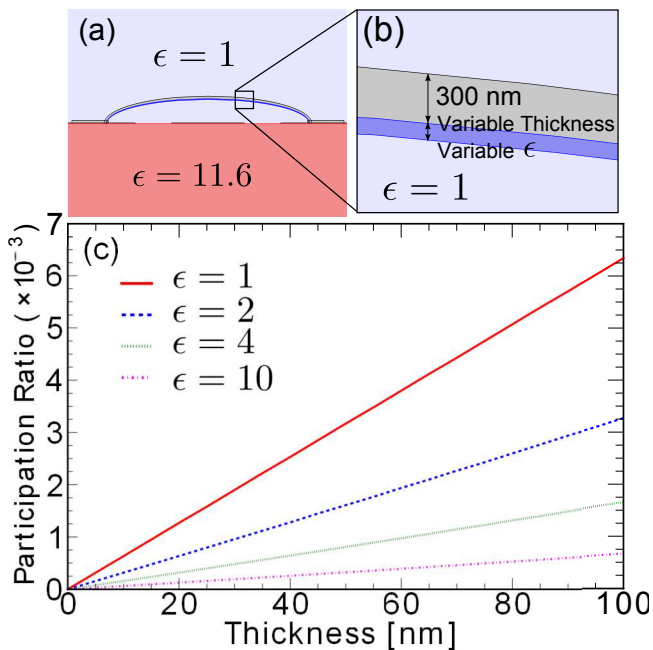


Figure 4. (Color online): (a) Cross section of an airbridge spanning a CPW line. (b) Close-up of the interface for which we calculate the participation ratio. This interface is a possible source of loss because the layer of aluminum is deposited on photoresist that has been crosslinked by an ion mill. The thickness and dielectric constant are variable. (c) Participation ratio as a function of thickness for various dielectric constants at the interface. We numerically calculate using COMSOL the participation ratio by setting the potential of the center trace of the CPW to 1V, solving for the electric fields, then numerically computing the integral in Eq. 1 in the interface region. We obtain the total energy  $W$  by performing the same integral for all of the cross section.

inductance and capacitance per unit length,  $LC$ , which is shown in Fig. 3(b). The slope of the linear fit in Fig. 3(b) indicates that the  $LC$  product for a section of line covered by airbridge differs from the bare line by 12.7%.

The discrepancy between our prediction and our data is most likely due to changes in the inductance of the resonator. Each airbridge adds additional pathways for current to flow, which decreases the inductance of the CPW line and compensates in part for the increase in capacitance. However, the inductance is not as easily modeled as the capacitance since edge effects are important. In other words, a single, wide airbridge that spanning a CPW line does not have the same effect as multiple narrower airbridges because they contain different current paths.

#### IV. PARTICIPATION RATIO OF THE AIRBRIDGE INTERFACE

The interface underneath the airbridge is a potential source of loss, since this is the interface at which

we deposited aluminum on photoresist that has been crosslinked by the argon ion mill. To understand the additional surface loss due to this interface, we calculate the participation ratio of a lossy dielectric at this metal-air interface following Ref 6. We consider the resonator and airbridge structure in cross section as shown in Fig. 4(a). The participation ratio  $p$  of any isotropic region of space in this cross-section is simply given by the ratio of energy stored in the region to the total energy stored in the entire cross-section

$$p = W^{-1} \epsilon_r \epsilon_0 \iint dA \frac{|E|^2}{2} \quad (2)$$

where  $W$  is the total energy in the cross-section which may be obtained by performing the same integral over all space, and  $\epsilon_r$  is the dielectric constant in the region. Assuming that the region is thin, as it is in the case of our interface of interest, we can replace an integral over the thickness by a product, turning the double integral into a line integral over the boundary of the interface. We can also simplify the equation using the boundary conditions on our interface. The metal boundary allows us to approximate the electric field as normal to the metal, while the continuity of the displacement field at the air interface gives us the relation  $\epsilon_r E_{i\perp} = E_{a\perp}$ , where  $E_i$  is the electric field in the interface and  $E_a$  is the electric field in air. Combining these simplifications we obtain

$$p = W^{-1} t_i \epsilon_r^{-1} \epsilon_0 \int dS \frac{|E_{a\perp}|^2}{2} \quad (3)$$

where  $t_i$  is the small thickness of the interface. Assuming the contribution to the total energy  $W$  of the interface is small, the participation ratio is proportional to the thickness and inversely proportional to the dielectric constant. We can estimate the value of the line integral by again modeling the airbridge as a parallel plate. If we assume a 1V difference in potential between center trace and ground, then from the calculation of total capacitance above, we know the value of  $W = \frac{1}{2} CV^2$ . The electric field is given by 1V divided by the separation distance of  $3 \mu\text{m}$ , and we may replace the integral with a multiplication by the length, about  $10 \mu\text{m}$ . We then obtain the following approximate formula:

$$p = 4.8 \times 10^{-5} \text{ nm}^{-1} \frac{t_i}{\epsilon_r} \quad (4)$$

Alternatively, we can also numerically evaluate Eq. 1. We constructed the geometry of an airbridge spanning a CPW and included a thin dielectric interface on the underside of the bridge as shown in Fig. 4(b). After applying a potential of 1V to the center trace, we solved for the electric fields and numerically integrated Eq. 1 to determine the total energy in the cross-section and the energy in the interface, giving us the participation ratio. We calculated participation ratio as a function of interface thickness and dielectric constant, producing the plot shown in Fig. 4(c). We see that the scaling follows the

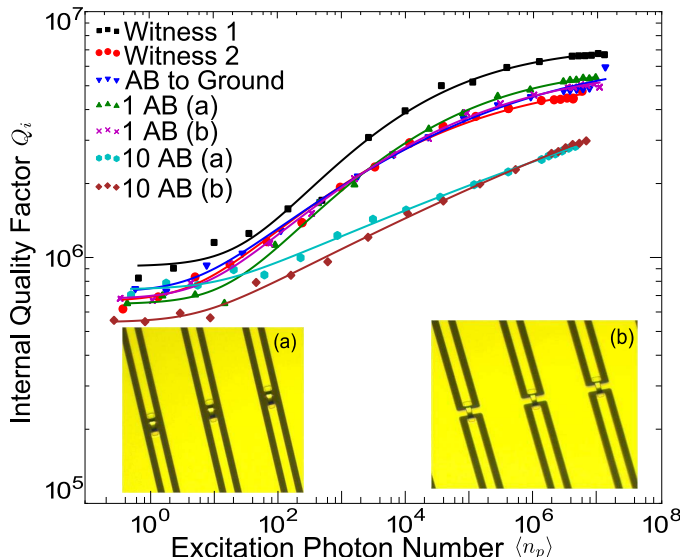


Figure 5. (Color online): Insets: (a) Airbridges connecting together CPW lines within a resonator. (b) A second style of airbridge connection, where the ground plane is threaded underneath the airbridge. Main panel: Internal quality factor of resonators as a function of average photon population for many different styles of resonators. We show two witness resonators to demonstrate the typical spread in measured  $Q_i$ . Lines are guides for the eye.

expected scaling from Eqs. 2 and 3. Furthermore, we can more accurately determine the coefficient in Eq. 3 from the slopes of the lines, and we find that the coefficient is  $6.34 \times 10^{-5} \text{ nm}^{-1}$ , which is within 30% of our parallel plate estimation.

Given the participation ratio, we can estimate the loss due to this interface. For the dielectric constant, we estimate a dielectric constant of 4 based on data pertaining to other photoresists<sup>7</sup>. SEM images of the interface were inconclusive for determining the thickness, but it is certainly upper bounded by 100 nm. Finally, there is little data on the loss tangent of resist and cryogenic temperatures, so we estimate this to be  $10^{-3}$  based on the measured loss tangents of amorphous oxides.<sup>8</sup> Using these numbers, we obtain a participation ratio of  $1.6 \times 10^{-3}$  and a loss due to airbridges of  $1.6 \times 10^{-6}$ , or a  $Q_i$  of 630,000.

## V. LOSS DUE TO INLINE AIRBRIDGES

Given the high critical currents through the airbridges, we know that the airbridges provide a good connection at DC. In order to test connectivity at microwave frequencies, we fabricated airbridges as a part of the center trace of the quarter wave resonators described in the main paper. We considered two styles of inline airbridges. In

both styles, we design the center trace to have a  $20 \mu\text{m}$  break, then connect together the two traces with an airbridge. In one style shown in Fig. 5(a), the ground plane is left unconnected, while in the other style shown in Fig. 5(b), the ground plane is connected through the break in the center trace and underneath the bridge.

We tested one and ten inline airbridges placed inside quarter wave CPW resonators in both styles. In addition, we tested a quarter wave resonator with an inline airbridge acting as the short to ground, since this configuration gave the largest current loading of the airbridge. Based on loss results in the main paper, we were confident that the airbridge processing did not degrade the quality factors of our resonators and used witness resonators fabricated on the same chip as the control resonators. All resonators had a larger center trace of  $15 \mu\text{m}$  to accommodate the pads of the bridge, a gap of  $10 \mu\text{m}$ , and were fabricated using aluminum deposited on a sapphire substrate. We performed quality factor measurements as described in the main paper, producing the results shown in Fig. 5.

The two witness resonators shown in Fig. 5 represent the best and worst measured quality factors for our witness resonators. On average, the witness resonators show a low power  $Q_i$  of around 800,000, and a high power  $Q_i$  of around  $5 \times 10^6$ . All resonators which have a single inline airbridge, including the resonator shorted to ground by the airbridge, do not show substantial degradation in  $Q_i$ . On the other hand, ten inline airbridges shows some degradation at high power corresponding to an additional loss of  $3 \times 10^{-7}$ . Ten inline airbridges with threaded ground planes also showed significant loss at lower power, with an additional loss of  $1.3 \times 10^{-6}$ , or  $10^{-7}$  per bridge.

## REFERENCES

- <sup>a</sup>Electronic mail: martinis@physics.ucsb.edu
- <sup>1</sup>R. Barends, J. Kelly, A. Megrant, D. Sank, E. Jeffrey, Y. Chen, Y. Yin, B. Chiaro, J. Mutus, C. Neill, et al., *Phys. Rev. Lett.* **111**, 080502 (2013).
- <sup>2</sup>R. Barends, J. Kelly, A. Megrant, A. Veitia, D. Sank, E. Jeffrey, T. C. White, J. Mutus, A. Fowler, B. Campbell, et al. (2014), in preparation.
- <sup>3</sup>M. Tinkham, *Introduction to Superconductivity* (Dover Publications, 2004), 2nd ed.
- <sup>4</sup>W. Skocpol, *Phys. Rev. B* **14**, 1045 (1976).
- <sup>5</sup>J. Romijn, T. Klapwijk, M. Renne, and J. Mooij, *Physical Review B* **26**, 3648 (1982).
- <sup>6</sup>J. Wenner, R. Barends, R. Bialczak, Y. Chen, J. Kelly, E. Lucero, M. Mariantoni, A. Megrant, P. O'Malley, D. Sank, et al., *Appl. Phys. Lett.* **99**, 113513 (2011).
- <sup>7</sup>J. Pierce and J. Pritchard Jr, *Component Parts*, *IEEE Transactions on* **12**, 8 (1965).
- <sup>8</sup>A. D. O'Connell, M. Ansmann, R. Bialczak, M. Hofheinz, N. Katz, E. Lucero, C. McKenney, M. Neeley, H. Wang, E. Weig, et al., *Appl. Phys. Lett.* **92**, 112903 (2008).